

# X-ray emission of the Be star/pulsar system PSR B1259–63 at non-periastron phases

Yuki ONO,<sup>1</sup> Yoichi YATSU,<sup>1</sup> Mikio MORII,<sup>2</sup>  
Nobuyuki KAWAI<sup>1</sup> and the MAXI team

<sup>1</sup> Department of Physics, Tokyo Institute of Technology, 2-12-1, Ohokayama, Meguro, Tokyo, Japan

<sup>2</sup> The Institute of Statistical Mathematics, 10-3-D414, Midoricho, Tachikawa, Tokyo, Japan

*E-mail*(YO): *onoy@hp.phys.titech.ac.jp*

## ABSTRACT

We report on the MAXI observation of the field of PSR B1259–63. X-ray flares have been observed at orbital phases far from the periastron. However, IGR J13020–6359 is located at 0.16 deg from PSR B1259–63, making it difficult to identify the sources of the flares. In this study, we fit the X-ray images with the Point Spread Function of MAXI GSC to determine the position of the X-ray flares accurately. As a result, we can distinguish the flares of PSR B1259–63 from those of IGR J13020–6359; three flares out of five flares are likely to be from PSR B1259–63. We suggest that its Be star companion temporarily releases a large amount of gas in directions other than the circumstellar disk, resulting in increases of the stellar wind density around the pulsar at phases far from the periastron.

KEY WORDS: pulsars: individual(PSR B1259–63) — X-rays: binaries

## 1. Introduction

PSR B1259–63/SS 2883 is a binary system in which a pulsar orbits around a Be star with a long orbital period of about 3.4 year. It is argued that the system is non-accreting and a shock is formed between the pulsar wind and the Be star wind, resulting in particle acceleration and non-thermal high energy emission near periastron out to TeV gamma-ray bands (Tavani et al. 1997).

## 2. Observation

Figure 1 is the X-ray light curves of the field of PSR B1259–63. According to Figure 1, X-ray flares have been observed at orbital phases far from the periastron. However, the resolution of MAXI GSC is typically on the order of 1.5 deg, while a nearby transient source IGR J13020–6359 is located at 0.16 deg from PSR B1259–63, making it difficult to identify the sources of the flares.

The source of Flare 1 is identified as IGR J13020–6359 by Swift/XRT observation (Kong et al. 2010) and the source of Flare 2–5 has not been identified due to lack of concurrent XRT observation.

## 3. Analysis and results

In order to identify the source of the flares, we determined the position of the X-ray flares with using the PSF fit tools (Morii et al. 2016). We formed a PSF model

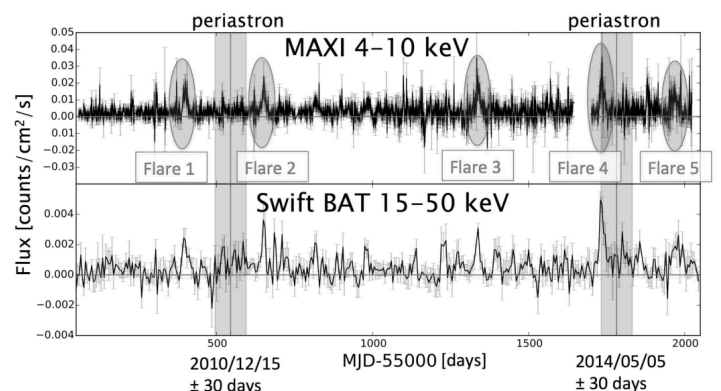


Fig. 1. MAXI/GSC and Swift/BAT light curves of the field of PSR B1259–63. The upper panel shows the MAXI GSC light curve and the lower panel shows the Swift BAT light curve. Periastrons and flares are highlighted with shades.

consisting of a flare source, catalogued X-ray sources excluding PSR B1259–63 and IGR J13020–6359, and background photons on a detector coordinate of MAXI GSC. We then allowed the position of the flare source to move and determined its position to maximize the likelihood function. Figure 2 is the results of the PSF fit determining the position of the X-ray flares. Fig-

Flare ID	orbital phase $\phi$	Flux (1-20 keV) $\times 10^{-10}$ erg cm $^{-2}$ s $^{-1}$	$L_{1-20\text{keV}}$ $\times 10^{35}$ [erg cm $^{-2}$ s $^{-1}$ ]
Flare 2	0.085	$2.81^{+0.51}_{-0.60}$	$1.77^{+0.32}_{-0.37}$
Flare 3	0.641	$4.76^{+0.50}_{-0.71}$	$3.00^{+0.32}_{-0.45}$
Flare 4	0.962	$7.41^{+0.50}_{-2.31}$	$4.67^{+0.32}_{-1.46}$
Flare 5	0.148	$3.83^{+0.21}_{-0.73}$	$2.42^{+0.13}_{-0.46}$

Table 1. A list of the flux and the luminosity of the observed flares. We assumed that PSR B1259–63 is located at a distance of 2.3 kpc.

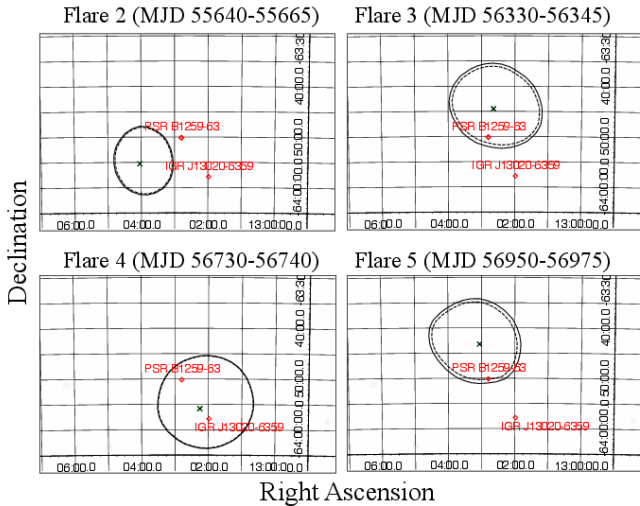


Fig. 2. The calculated position of the flares with using the PSF fit tool. The cross marks show the calculated position. The dashed lines show that the statistical 90 % confidence level. The solid lines show that the 90 % confidence level taking the systematic error of MAXI GSC into account.

Figure 2 shows that the source of three flares out of four flares are consistent with PSR B1259–63 (Flare 2, 3, 5). The position of the flare 4 is near IGR J13020–6359 but contains the coordinates of both IGR J13020–6359 and PSR B1259–63. Therefore, we included the flare 4 in discussion.

#### 4. Discussion

We assumed that synchrotron cooling dominates the emission of these flares from the shocked wind and that the shocked electron pairs have a power-law distribution  $N(\gamma) = K\gamma^{-p}$  ( $\gamma_{\min} < \gamma < \gamma_{\max}$ ). We then calculated the X-ray luminosity emitted from the shock-accelerated electron/positron (Murata et al. 2003). The parameters we used for the calculations are the minimum Lorentz factor  $\gamma_{\min}$ , the power law index  $p$ , the conversion efficiency from the pulsar spin-down luminosity to the relativistic electron/positron pairs  $\epsilon_a$ , and the ratio of the shock distance from the pulsar to the binary separation

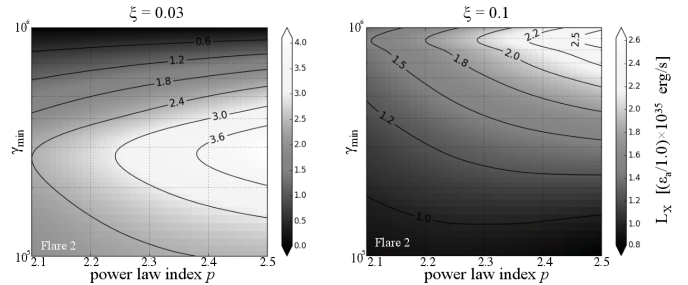


Fig. 3. The calculation results of the X-ray luminosity.

$\xi$	Flare 2	Flare 3	Flare 4	Flare 5
0.03	46.7	161.5	12.0	108.3
0.05	16.1	55.3	4.13	37.6
0.08	5.92	20.4	1.51	13.6
0.1	3.63	12.1	0.929	8.23

Table 2. The mass loss rate of the spherically symmetric Be star outflow  $\dot{M}$  with each  $\xi$ . The mass loss rates  $\dot{M}$  in the table is given in units of  $10^{-6} M_{\odot}/\text{yr}$ .

$\xi$ . We found that the observed flux can be explained when  $\epsilon_a$  is  $\sim 0.8$  and  $\xi$  is  $< 0.1$  (Figure 3).

We suggest that the Be star temporarily releases a large amount of gas in directions other than the circumstellar disk, resulting in increases of the stellar wind density around the pulsar at phases far from the periastron. When we assume that the Be star wind is spherically symmetric, such a small shock distance is possible when a mass loss rate of the Be star  $\dot{M}$  is  $10^{-4} - 10^{-6} M_{\odot}/\text{yr}$  (Table 2).

#### References

- Sugizaki et al. 2011, PASJ, 63, 635
- Mihara et al. 2011, PASJ, 63, S623-S634
- Tavani & Arons 1997, ApJ, 477, 439-464
- Murata et al. 2003, PASJ, 55, 473-481
- Morii et al. 2016, PASJ, 68, S11
- Kong et al. 2010, ATEL #2782